Published in final edited form as:
J Orthop Res. 2012 September ; 30(9): 1413–1422. doi:10.1002/jor.22087.

Changes Induced by Chronic *in vivo* Load Alteration in the Tibiofemoral Joint of Mature Rabbits

Maria L. Roemhildt[*], **Bruce D. Beynnon**[*], **Mack Gardner-Morse**[*], **Gary Badger**[#], and **Calsey Grant**[*]

[*]McClure Musculoskeletal Research Center, Department of Orthopaedics and Rehabilitation, College of Medicine, University of Vermont

[#]Department of Medical Biostatistics, University of Vermont

Summary

We investigated the relationship between the magnitude and duration of chronic compressive load alteration and the development and progression of degenerative changes in the rabbit tibiofemoral joint. Varus loading devices were attached to the hind limb of mature NZW rabbits. Altered compressive loads of 0, 50 and 80% body weight (BW) were applied to the tibiofemoral joint for 12 hours per day for 12 and 24 weeks (n=4 animals/group). Compartment-specific assessment of the tibial plateau included histological assessments (articular cartilage, calcified cartilage, and subchondral bone thicknesses, degeneration score, and articular cartilage cellularity) and biomechanical measures (aggregate modulus, permeability, Poisson's ratio). Analyses of variance techniques were used to examine the relationship between each outcome measure with load magnitude and duration as independent variables in the model. Degenerative changes developed in the medial compartment with increased magnitude of compressive loading and included fibrillation, increased degeneration score, and reduced cellularity of the articular cartilage. Increased calcified cartilage thickness was observed in both the medial and lateral compartments following exposure to altered loading of 80% BW for 24 weeks. This work demonstrates that *in vivo* chronic compressive load alteration to the tibiofemoral joint can initiate progressive macroscopic and histological-based degenerative changes analogous to the early changes occurring in OA.

Keywords

cartilage degeneration; animal model; mechanical loading; osteoarthritis

Introduction

Osteoarthritis (OA) is a heterogeneous group of disorders that result in degeneration of articular cartilage and modification of joint structures. Clinically, knee malalignment and increased BMI are associated with development of primary OA (1,2) and increased articular contact stresses are predictive of OA development (3). Osteotomy or wedged insoles are used to treat unicompartmental OA by redistributing loading across the knee (4,5). Despite acceptance that aberrant mechanical loads play a role, *in vivo* quantitative assessments of the mechanisms by which articular cartilage responds to sustained compressive loading are

Corresponding author: Maria Roemhildt, Ph.D. University of Vermont 428 Stafford Hall 95 Carrigan Drive Burlington, VT 05405, USA Tel: 1-802-656-3823 Fax: 1-802-656-4247 maria.roemhildt@med.uvm.edu.

The authors of this work have no conflicts of interest.

limited (6). Although requisite loading maintains cartilage homeostasis and abnormal loading levels result in cell death and matrix degradation, the thresholds of non-injurious chronic-load levels and the role of chronic-load alteration in the development of OA have yet to be elucidated (7,8).

Animal models incorporating osteotomy, external loading devices, immobilization, forced exercise, and/or transection of joint structures have been used to investigate the effects of load alteration on articular joints and its contribution to degenerative changes (9,10). In these models, the load alteration and resulting change in contact stress experienced by the cartilage remains challenging to control and quantify, which may contribute to the range of treatment effects observed. For example, although strenuous running in rats produces osteoarthritic changes with a dose response relationship and increased severity when combined with ACL-transection (11–14), strenuous running in humans and canines is typically well tolerated (15,16). In one long-term study, no deleterious effects of lifelong exercise were observed even when dogs wore weighted vests (16). Existing animal models of OA that are based on ligament and meniscus transection or injection of degradative agents disrupt the joint capsule, alter loading in an undocumented manner, and typically result in rapid development of degenerative joint changes unlike primary OA in humans, which develops over many years. Changes occurring in joint tissues during the early stages of knee OA in which mechanical loads play an etiologic role are not fully understood.

A varus loading device (VLD) was previously developed to apply a varus moment to the rabbit tibiofemoral joint that results in a controlled increased load to the medial compartment and equivalent decreased load in the lateral compartment without disruption of the joint capsule while maintaining normal use of the joint (17). The altered load can be removed by disengaging the device, and the change in load is quantifiable and can be modulated in a controlled manner. Use of the VLD model allows the role of altered loading to be isolated, and its contributions to the onset and development of joint disease to be evaluated *in vivo.*

In our previous study, chronic load increase of 44% body weight (BW) applied to the medial compartment of the rabbit knee for 12 wks resulted in increased articular cartilage thickness and permeability, but minimal fibrillation of the articular surface (17). It remains to be determined if load-induced changes progress with increased loading duration, accelerate with increased loading magnitudes, or initiate gross degenerative changes. This motivated us to investigate the relationship between the magnitude and duration of chronic load alteration and the development of degenerative changes using histological, mechanical, and biochemical assessments. We hypothesized that the level of joint degeneration (as quantified by histological measures and cartilage material properties) would increase with increasing magnitudes of applied altered compressive loading (0, 50, and 80% BW) and duration (12 and 24 wks).

Methods

Animal model

20 male, skeletally-mature, NZW rabbits, ~12 mos of age, mean weight (± SD) of 4.46 (± 0.48) kg were randomized into one of 5 treatment groups: 0% BW-12 wks (Sham), 50% BW-12 wks, 80% BW-12 wks, 50% BW-24 wks, and 80% BW-24 wks (n=4 animals/group). The study was approved by the University of Vermont's Animal Care and Use Committee. Animals were housed in cages 62 × 76 cm with polycarbonate flooring, given food (Purina chow 5321/5326) and water *ad libitum*, and maintained on a 12:12 hr light/dark cycle. Animals underwent unilateral surgery to implant custom stainless steel bone plates on the lateral aspect of the femur and tibia as previously described (17). After 10 days of

recovery, animals were briefly anesthetized, the VLD was attached to the plates, and the rotational axis of the VLD was aligned with the femoral transepicondylar axis using fluoroscopy (Fig 1). The varus force at the tibia (F) required to produced the target overload of the medial compartment (ΔP) was calculated from the equation, $F=\frac{\Delta P * D}{L}$, where D = intercompartmental moment arm, and L = tibia moment arm (17). A hand-held force gauge (FGE-2.0, Shimpo, Kyoto Japan) was used to measure F.

Animals were exposed to one of the 3 loading levels for 12 hrs/day (7AM – 7PM) over 12 or 24 wks. Loading was initiated 14 days post surgery using a 5 day ramp-up period in which the load was incrementally increased by 20% of the target load each day. Load levels were measured at the start and end of each daily loading period and adjusted if not within ± 10% of the target load. Animals were active within their cages with full range of motion of the tibiofemoral joint.

Animals were euthanized at completion of the loading interval, and a serum sample collected. Synovial fluid lavage was aspirated from the knee following injection of 1.5 mL of sterile saline and 10 flexion-extension cycles (18). Tibial plateaus were excised from experimental and contralateral limbs, digital images of each specimen were collected, and the cartilage surfaces evaluated for macroscopic changes following staining with India ink using a 4-point grading scale (1 = intact surface, 2 = minimal fibrillation, 3 = overt fibrillation, and 4 = erosion) (19). Additionally, qualitative assessment of joint fibrosis and changes to the meniscus and ligament structures were noted. Specimens were stored at −80°C until testing.

Mechanical Evaluation

Cartilage material properties (aggregate modulus, permeability, and Poisson's ratio) were determined using biphasic creep-indentation (20,21); a needle probe was used to determine cartilage thickness at the test location (22). Central and posterior sites were evaluated in the medial compartment and a central site in the lateral compartment of the tibial plateaus in experimental and contralateral limbs (Fig. 2A). Testing locations were selected to represent regions with direct contact between the femoral and tibial cartilage at paw-strike during hopping (Center) and while seated (Posterior) (17). Specimens were thawed in a saline bath with protease inhibitors prior to testing. Indentation was performed with a cylindrical, plane-ended, porous, 1.0 mm diam indenter, 0.044 MPa tare load, and 0.125 MPa test load using a custom device (23). An arthroscope (~10× mag.) was used to confirm positioning and alignment of the cartilage surface normal to the loading axis of the indenter. Material properties were determined by curve-fitting the load-displacement response with the biphasic indentation creep solution using nonlinear regression (21). The mean ± SD strain across all specimens was 3.43 ± 2.21%.

Histologic Evaluation

Two 2 mm coronal sections were prepared from each plateau, fixed in 10% buffered formalin, decalcified in 10% EDTA, paraffin embedded, and microtomed at 7 μm, prior to staining with 0.5% w/v Safranin-O in 0.1 M phosphate and 0.1% Fast-Green (SOFG) and with Hemalotoxylin and Eosin (H&E) (24,25) (Fig. 2A). Slides were examined under light microscopy (BX50, Olympus Inc.) with digital images of the medial and lateral compartments collected (1200 × 1600 pixels) (RET-2000R-F-CLR-12-C, QImaging).

Cartilage degeneration was evaluated on SOFG stained slides using a modified Mankin grading system for assessment of OA in the rabbit (19). The semiquantitative score is based on 4 parameters: staining intensity (0–6), cartilage structure (0–11), chondrocyte density (0–

4), and cluster formation (0–3), with aggregate scores ranging from 0 to 24 (Supplemental Table 1).

Articular cartilage, calcified cartilage, and subchondral bone thicknesses were measured across each compartment on digital images of SOFG stained slides (Fig. 2B). Briefly, a 3 × 2.2 mm central region of interest (ROI) was defined that excluded extreme axial and abaxial areas (26). The articular surface, tidemark, calcified cartilage-subchondral bone junction, and inferior boundary of the subchondral bone plate were identified at 60 equally spaced points across each compartment using custom written Matlab code to determine thicknesses and articular cartilage area. Area measurements were subdivided into 4 equally spaced regions across the width of the ROI (peripheral, peripheral-central, midline-central, and midline) and 3 zonal-depths (superficial (0–25%), mid (25–50%), and deep (50–100%), Fig. 2C).

Articular cartilage cellularity was determined by counting chondrocytes with visible nuclei in H&E stained sections across the ROI with measurements subdivided as in the area measurements. Cellularity was determined as the number of chondrocytes/area of articular cartilage. Digital images illustrating nuclei are provided in Supplemental data (Figs. S1 & S2).

Synovial Fluid Glycosaminoglycan

The concentration of sulfated-glycosaminoglycans in synovial fluid lavage was determined using the Alcian blue quantitative dye-binding assay (sGAG, Alpco Diagnostics, Salem, NH)(27). The urea contents of the lavage and serum were measured (Quantichom Urea Assay Kit DIUR-500, BioAssay Systems, Hayward, CA) and used to determine the dilution factor of the lavage sample (28).

Statistical analyses

ANOVAs were used to model the relationship between each outcome measure (material properties, histological assessment, GAG content) of the experimental limb and the controlled variables (load magnitude and load duration). Due to the unbalanced nature of the study design, contrasts were used to examine main effects of load magnitude, load duration, and their interaction. *A priori* contrasts were also used to examine simple effects of magnitude and duration (eg. magnitude effect within a given loading duration or duration effect within a given load level). Group means (+ standard error) are presented in plots of the results. Comparisons with p-value ≤ 0.05 were considered significant. Percentage differences in outcome measures were calculated as (observed value - reference value)/ reference value * 100.

Results

Gross observations

Specimens from all groups showed fibrillation in the medial compartment and intact surfaces in the lateral compartment (Fig 3). Modified Mankin scores increased in the medial compartment with each loaded group being significantly different from the 0% BW-12 wks (Sham) group ($p<0.01$; Fig 4). No other differences were observed across groups. No differences across groups were observed for the score in the lateral compartment. Qualitatively, hypertrophy of the lateral collateral ligament, separation of fiber bundles of the posterior cruciate ligament, and fibrosis of the joint were observed with increased loading (Supplement Fig. S5).

Histological Evaluation

The mean degeneration score in the medial compartment differed significantly across groups (p=0.01) and with time (p=0.01; Figs. 3 & 4). The mean score in the 80% BW-24 wks group increased 110% in comparison to the 0% BW-12 wks (Sham) group (p<0.01) and 58% compared to the 80% BW-12 wks group (p=0.01). Similarly the 50% BW-12 and 50% BW-24 wks groups were each increased 60% as compared to the 0% BW-12wks group (p=0.04 each). A significant effect of time on degeneration score was observed in the lateral compartment with the score in the loaded (50 & 80% BW) groups significantly increased at 24 wks compared to loaded groups at 12 wks (p=0.03).

The mean cellularity varied with time across groups in the medial compartment (p=0.01; Figs. 3 & 4). Cellularity of the 50% BW-24 wks group was decreased 22% as compared to the 50% BW-12 wks group (p=0.03). A trend for a similar decrease of 22 % was observed for the 80% BW-24 wks group as compared to the 80% BW-12 wks group (p=0.08). Regional changes in cellularity were observed in the midline region of the plateau and the superficial zone (Suppl. Figs. S3 & S4). No overall effects were observed for cellularity of the lateral compartment.

The thickness of the calcified cartilage in the medial compartment of the 80% BW-24 wks group was increased 61% as compared to 0% BW-12 wks and 56% as compared to 50% BW-24 wks values (p=0.05 each; Fig. 5). In the lateral compartment, the calcified cartilage thickness of the 80% BW-24 wks group was also increased (45–70%) as compared to 0% BW-12 wks (p=0.03), 80% BW-12 wks (p=0.05), and 50% BW-24 wks groups (p=0.03). The thickness of the articular cartilage in the lateral compartment of the 50% BW groups showed a trend to vary with time (p=0.10) with the thickness increased 44% in the 24 wks group as compared to 12 wks (p=0.05). No significant differences across groups were detected for articular cartilage thickness in the medial compartment or subchondral bone thickness in either the medial or lateral compartments.

Mechanical Evaluation

In the medial compartment at the posterior test location, the Poisson's ratio varied significantly with load level (p=0.01) with a trend with group (p=0.06) (Fig 6). The Poisson's ratio of the 50% BW loaded groups was reduced as compared to 0% BW-12 wks group (p=0.04). The Poison's ratio of the 50% BW-24 wks group was decreased as compared to 0% BW-12 wks (p=0.05) and 80% BW-24 wks (p=0.02) groups. The aggregate modulus of the 50% BW loaded groups was decreased as compared to the 0% BW-12 wks group (p=0.08). Although the mean aggregate modulus of the 50% BW groups was elevated over the 80% BW groups, this difference did not reach significance. The permeability was elevated at 24 wks as compared to 12 wks, but did not reach significance. No differences for aggregate modulus, permeability, or Poisson's ratio were observed across groups in the central location of either plateau.

Synovial Fluid Glycosaminoglycan

The concentration of glycosaminoglycan in synovial fluid of the tibiofemoral joint did not vary significantly across experimental groups (Fig. 7).

Discussion

In vivo chronic compressive load alteration applied to the rabbit tibiofemoral joint initiated degenerative changes as evidenced by macroscopic cartilage fibrillation, increased degenerative scoring, and diminished cellularity. These changes were most pronounced in the medial compartment which experienced increased compressive loading. Increased

calcified cartilage thickness was observed both the medial and lateral compartments. Histological-based metrics of degeneration detected the alterations before significant effects on material properties.

The diminished cartilage cellularity observed in the medial compartment at 24 wks as compared to 12 wks is consistent with chondrocyte loss that occurs early in human OA (29,30) and leads to alterations in cartilage matrix production and load-bearing capacity. Hypertrophy of the chondrocytes was observed in the loaded groups, most prominently in the 80% BW-24 wks group (Fig 3-N). Chondrocyte hypertrophy and chondron enlargement were observed in early human OA and may be related to attempts to repair damaged cartilage (31,32). Diminished cellularity and changes to chondrocyte morphology were also reported in the rabbit knee 12 wks after ACL-transection (33). We did not evaluate the mechanism of cell death; investigations in rat OA models suggest both apoptotic and authophagy pathways (34–36). Lower cartilage cellularity in the medial as compared to the lateral compartment was also observed in mature rats (37) and may decrease the ability of the cartilage to accommodate the applied levels of altered loading.

The OARSI recommendations for histological assessment of rabbit OA were used (19); these guidelines were developed to provide a standardized system for assessing joint instability models in which degenerative changes develop within weeks. In our study, the degeneration score in the medial compartment of the loaded groups ranged from 4.0–6.25 indicating mild degeneration and more slowly developing changes as compared to ligament and meniscus transection models (16). The changes we observed may be similar in severity to early degenerative changes observed with strenuous exercise in rats (11,38). Different pathoetiologies may exist for each model; our model provides an alternative to study controlled and quantifiable levels of chronic load alteration in which degenerative changes develop slowly and may provide additional insight into the disease processes associated with non-traumatic OA in which mechanical loads play a key role in onset and early progression.

An increase in articular cartilage thickness was observed in early OA (39) and is thought to result from swelling of the cartilage matrix stemming from decreased proteoglycan content and disruption of the collagen fibrils (40). In the lateral compartment, cartilage thickness increased in the 50% BW-24 wks group over the 50% BW-12 wks group, and in the medial compartment a similar trend was observed (Fig. 5). In animal studies using altered loading following joint immobilization, no change in compressive modulus was observed up to 8 wks (41,42); however, with increased duration of incomplete immobilization, irreversible cartilage softening was observed (43). Furthermore, decreased load was associated with increased proteoglycan and collagen content while increased load decreased proteoglycan and collagen content in a guinea pig where load alteration was induced by valgus femoral osteotomy (44). Articular cartilage thinning is observed following reduced joint loading after spinal cord injury (45), whereas increased cartilage thickness is observed with unloading via joint distraction (46).

Increased calcified cartilage thickness was observed in both compartments in the 80% BW-24 wks group. Increased thickness was also observed with moderate and severe OA in canines (47) and rabbits exposed to blunt impact of the tibiofemoral joint (48). Calcified cartilage is thought be quiescent in adults; however, it may be reactivated in OA with further cartilage mineralization (49).

Load-induced changes to mechanical properties were most prominent in the posterior location of the medial compartment, corresponding to the location of tibiofemoral contact when the rabbit is sitting. Load-induced changes in this location are consistent with the location of greatest treatment effect in our prior work (17). Similarly, localized degenerative

changes to the posterior region of the medial compartment were observed in the rabbit ACL transection model (50). Since regional variation of material properties in the rabbit tibial plateau was previously shown (23), we focused on analyses across experimental groups within each location.

Other alterations in joint were observed, including ligamentous changes and fibrosis (Suppl. Fig. S5). These observations were most evident in the experimental limb of the 80% BW-24 wk group. Regions of focal necrotic lesions were observed within the articular cartilage across all groups (Suppl. Fig. S6). These acellular regions were morphologically consistent to regions of mineralized cartilage previously reported in animal models (51, 52) and human cartilage (53).

Based on prior work that investigated altered loads of 22 and 44% BW at 12 wks (17), we hypothesized that a higher load level (80% BW) and longer duration (24 wks) would create more severe changes to the joint tissues; however, this was not observed. Changes in the flooring used in the cages (polycarbonate floor vs. metal grate), the use of males vs. females, or the ramp-up period during load application may have affected the response (17).

An *a priori* power calculation based on prior material property data indicated that 4 animals/group would be adequate. However, this sample size resulted in limited power to detect significant differences among groups on additional histological- and biochemical-based outcomes. Minimal effects of aging were anticipated in these skeletally mature rabbits over a 12-wk period (54–56), so a 0% BW-24 wks group was not included.

We did not determine hind limb ground reaction forces. Alterations to hind limb load bearing may have been produced by attachment of the VLD, but was accounted for with the Sham group. In a rat model, application of altered loads via the VLD had no effect on vertical ground reaction force (57). Hind limb loading may diminish with development of degenerative joint disease; however, the mild/moderate focal changes we observed were much less severe than the stages of degeneration typically observed with more aggressive OA models OA (58–60).

This work demonstrates that the VLD rabbit model may be used to study an important risk factor associated with OA, increased loading. Overall, the combination of load levels (50% and 80% BW) and duration (12 and 24 wks) initiated degenerative changes in the medial compartment consistent with early OA. Additionally, increased calcified cartilage thickness and focal chondrocyte hypertrophy were observed with increased loading, suggesting that sustained altered compressive loads >50% BW applied for ≥12 wks may be beyond the thresholds that joint tissues can accommodate. Load-induced changes to chondrocyte metabolism may contribute to cell death that diminishes the capacity of the cartilage to maintain and repair extracellular matrix, thus resulting in proteoglycan loss and subsequent matrix erosion. During this process, degradative fragments would be released into the surrounding joint fluid that may elicit inflammation and contribute to the development of OA. In this study, histological outcomes were more sensitive to early load-induced changes than biomechanical properties, perhaps because the mechanical properties reflect bulk properties at the testing site while histology reveals more localized and depth-specific changes. The mechanisms by which load-induced chondrocyte death occurs in our model, whether these alterations may be self mitigating if the altered loading is removed, and whether the load threshold that initiates detrimental effects is modified with aging or systemic factors remain to be determined.

Supplementary Material

Refer to Web version on PubMed Central for supplementary material.

Acknowledgments

Funded by NIH-NIAMS: R-21 AR052815-01. The authors are grateful to Dr. Nelson Tacy, Amy Gassman, and Danielle Funaro for their assistance with experimental procedures and animal care, Kiley Anderson for providing analytical assistance, and Anna Gauthier for assistance in manuscript preparation.

References

1. Brouwer GM, Tol AWV, Bergink AP, et al. Association between valgus and varus alignment and the development and progression of radiographic osteoarthritis of the knee. Arthritis Rheum. 2007; 56:1204–1211. [PubMed: 17393449]
2. Felson DT, Anderson JJ, Naimark A, et al. Obesity and knee osteoarthritis. The Framingham Study. Ann Intern Med. 1988; 109:18–24. [PubMed: 3377350]
3. Segal NA, Anderson DD, Iyer KS, et al. Baseline articular contact stress levels predict incident symptomatic knee osteoarthritis development in the MOST cohort. J Orthop Res. 2009; 27:1562–1568. [PubMed: 19533741]
4. Hernigou P, Medevielle D, Debeyre J, Goutallier D. Proximal tibial osteotomy for osteoarthritis with varus deformity. A ten to thirteen-year follow-up study. The Journal of bone and joint surgery. 1987; 69:332–354. American volume. [PubMed: 3818700]
5. Bennell KL, Bowles K-A, Wang Y, et al. Higher dynamic medial knee load predicts greater cartilage loss over 12 months in medial knee osteoarthritis. Ann Rheum Dis. 2011
6. Bader DL, Salter DM, Chowdhury TT. Biomechanical Influence of Cartilage Homeostasis in Health and Disease. Arthritis. 2011; 2011
7. Guilak, F.; Hung, CT. Physical Regulation of Cartilage Metabolism. In: Mow, VC.; Huiskes, R., editors. Basic Orthopaedic Biomechanics and Mechano-Biology. 3rd ed.. Lippincott Williams & Wilkens; Philidelphia, PA: 2005. p. 259-300.
8. Carter DR, Beaupre GS, Wong M, et al. The mechanobiology of articular cartilage development and degeneration. Clin Orthop Relat Res. 2004:S69–77. [PubMed: 15480079]
9. Pritzker KP. Animal models for osteoarthritis: processes, problems and prospects. Ann Rheum Dis. 1994; 53:406–420. [PubMed: 8037500]
10. Little CB, Smith MM. Animal Models of Osteoarthritis. Current Rheumatology Reviews. 2008; 4:175–182.
11. Pap G, Eberhardt R, Stürmer I, et al. Development of Osteoarthritis in the Knee Joints of Wistar Rats After Strenuous Running Exercise in a Running Wheel by Intracranial Self-Stimulation. Pathology - Research and Practice. 1998; 194:41–47.
12. Lee Y, Park J, Yang S, et al. Evaluation of osteoarthritis induced by treadmill-running exercise using the modified Mankin and the new OARSI assessment system. Rheumatology International. 2011; 31:1571–1576. [PubMed: 20490805]
13. Galois L, Etienne S, Grossin L, et al. Dose-response relationship for exercise on severity of experimental osteoarthritis in rats: a pilot study. Osteoarthritis Cartilage. 2004; 12:779–786. [PubMed: 15450527]
14. Appleton CT, McErlain D, Pitelka V, et al. Forced mobilization accelerates pathogenesis: characterization of a preclinical surgical model of osteoarthritis. Arthritis Research & Therapy. 2007; 9:R13. [PubMed: 17284317]
15. Hunter DJ, Eckstein F. Exercise and osteoarthritis. Journal of Anatomy. 2009; 214:197–207. [PubMed: 19207981]
16. Newton PM, Mow VC, Gardner TR, et al. Winner of the 1996 Cabaud Award. The effect of lifelong exercise on canine articular cartilage. Am J Sports Med. 1997; 25:282–287. [PubMed: 9167804]
17. Roemhildt ML, Coughlin KM, Peura GD, et al. Effects of increased chronic loading on articular cartilage material properties in the Lapine tibio-femoral joint. J Biomech. 2010; 43:2301–2308. [PubMed: 20488444]

18. Lindhorst E, Wachsmuth L, Kimmig N, et al. Increase in degraded collagen type II in synovial fluid early in the rabbit meniscectomy model of osteoarthritis. Osteoarthritis Cartilage. 2005; 13:139–145. [PubMed: 15694575]
19. Laverty S, Girard CA, Williams JM, et al. The OARSI histopathology initiative -recommendations for histological assessments of osteoarthritis in the rabbit. Osteoarthritis Cartilage. 2010; 18:S53–S65. [PubMed: 20864023]
20. Mak AF, Lai WM, Mow VC. Biphasic indentation of articular cartilage--I. Theoretical analysis. J Biomech. 1987; 20:703–714. [PubMed: 3654668]
21. Mow VC, Gibbs MC, Lai WM, et al. Biphasic indentation of articular cartilage--II. A numerical algorithm and an experimental study. J Biomech. 1989; 22:853–861. [PubMed: 2613721]
22. Athanasiou KA, Rosenwasser MP, Buckwalter JA, et al. Interspecies comparisons of in situ intrinsic mechanical properties of distal femoral cartilage. J Orthop Res. 1991; 9:330–340. [PubMed: 2010837]
23. Roemhildt ML, Coughlin KM, Peura GD, et al. Material properties of articular cartilage in the rabbit tibial plateau. J Biomech. 2006; 39:2331–2337. [PubMed: 16168420]
24. Kiraly K, Lammi M, Arokoski J, et al. Safranin O reduces loss of glycosaminoglycans from bovine articular cartilage during histological specimen preparation. Histochemical Journal. 1996; 28:99–107. [PubMed: 8737291]
25. Schmitz N, Laverty S, Kraus VB, Aigner T. Basic methods in histopathology of joint tissues. Osteoarthritis Cartilage. 2010; 18:S113–S116. [PubMed: 20864017]
26. LaPrade RF, Wentorf FA, Olson EJ, Carlson CS. An In Vivo Injury Model of Posterolateral Knee Instability. The American Journal of Sports Medicine. 2006; 34:1313–1321. [PubMed: 16567454]
27. Bjornsson S. Simultaneous Preparation and Quantitation of Proteoglycans by Precipitation with Alcian Blue. Analytical Biochemistry. 1993; 210:282. [PubMed: 8512063]
28. Kraus VB, Huebner JL, Fink C, et al. Urea as a passive transport marker for arthritis biomarker studies. Arthritis & Rheumatism. 2002; 46:420–427. [PubMed: 11840444]
29. Meachim G, Collins DH. Cell Counts of Normal and Osteo-Arthritic Articular Cartilage in Relation to the Uptake of Sulphate (35SO4) in vitro. Ann Rheum Dis. 1962; 21:45–50. [PubMed: 14471899]
30. Vignon E, Arlot M, Vignon G. The cellularity of fibrillated articular cartilage. A comparative study of age-related and osteoarthrotic cartilage lesions from the human femoral head. Pathologie-biologie. 1977; 25:29–32. [PubMed: 322033]
31. Goldring MB, Otero M, Plumb DA, et al. Roles of inflammatory and anabolic cytokines in cartilage metabolism: signals and multiple effectors converge upon MMP-13 regulation in osteoarthritis. European cells & materials. 2011; 21:202–220. [PubMed: 21351054]
32. Poole CA. Review. Articular cartilage chondrons: form, function and failure. Journal of Anatomy. 1997; 191:1–13. [PubMed: 9279653]
33. Vignon E, Bejui J, Mathieu P, et al. Histological cartilage changes in a rabbit model of osteoarthritis. Journal of Rheumatology. 1987; 14:104–106. [PubMed: 3625662]
34. Almonte-Becerril M, Navarro-Garcia F, Gonzalez-Robles A, et al. Cell death of chondrocytes is a combination between apoptosis and autophagy during the pathogenesis of Osteoarthritis within an experimental model. Apoptosis. 2010; 15:631–638. [PubMed: 20091349]
35. Etienne S, Gaborit N, Henrionnet C, et al. Local induction of heat shock protein 70 (Hsp70) by proteasome inhibition confers chondroprotection during surgically induced osteoarthritis in the rat knee. Bio-Medical Materials & Engineering. 2008; 18:253–260. [PubMed: 19065031]
36. Kobayashi K, Mishima H, Hashimoto S, et al. Chondrocyte apoptosis and regional differential expression of nitric oxide in the medial meniscus following partial meniscectomy. J Orthop Res. 2001; 19:802–808. [PubMed: 11562124]
37. Roemhildt ML, Anderson K, Beynnon BD, Gardner-Morse M. 235 Region specific cellularity of articular cartilage in the tibial plateau of the mature spague-dawley rat. Osteoarthritis Cartilage. 2010; 18:S108–S108.
38. Ni G-X, Zhan L-Q, Gao M-Q, et al. Matrix metalloproteinase-3 inhibitor retards treadmill running-induced cartilage degradation in rats. Arthritis Research & Therapy. 2011; 13:R192. [PubMed: 22114772]

39. Calvo E, Palacios I, Delgado E, et al. Histopathological correlation of cartilage swelling detected by magnetic resonance imagine in early experimental osteoarthritis. Osteoarthritis Cartilage. 2004; 12:878–886. [PubMed: 15501403]
40. Hollander AP, Heathfield TF, Webber C, et al. Increased damage to type II collagen in osteoarthritic articular cartilage detected by a new immunoassay. Journal of Clinical Investigation. 1994; 93:1722–1732. [PubMed: 7512992]
41. Setton LA, Mow VC, Muller FJ, et al. Mechanical behavior and biochemical composition of canine knee cartilage following periods of joint disuse and disuse with remobilization. Osteoarthritis Cartilage. 1997; 5:1–16. [PubMed: 9010874]
42. Vanwanseele B, Lucchinetti E, Stüssi E. The effects of immobilization on the characteristics of articular cartilage: current concepts and future directions. Osteoarthritis Cartilage. 2002; 10:408–419. [PubMed: 12027542]
43. Haapala J, Arokoski J, Pirttimaki J, et al. Incomplete restoration of immobilization induced softening of young beagle knee articular cartilage after 50-week remobilization. Int J Sports Med. 2000; 21:76–81. [PubMed: 10683104]
44. Wei L, Hjerpe A, Brismar BH, Svensson O. Effect of load on articular cartilage matrix and the development of guinea-pig osteoarthritis. Osteoarthritis Cartilage. 2001; 9:447–453. [PubMed: 11467893]
45. Vanwanseele B, Eckstein F, Knecht H, et al. Knee cartilage of spinal cord–injured patients displays progressive thinning in the absence of normal joint loading and movement. Arthritis Rheum. 2002; 46:2073–2078. [PubMed: 12209511]
46. Intema F, Van Roermund PM, Marijnissen ACA, et al. Tissue structure modification in knee osteoarthritis by use of joint distraction: an open 1-year pilot study. Ann Rheum Dis. 2011
47. Daubs BM, Markel MD, Manley PA. Histomorphometric analysis of articular cartilage, zone of calcified cartilage, and subchondral bone plate in femoral heads from clinically normal dogs and dogs with moderate or severe osteoarthritis. American Journal of Veterinary Research. 2006; 67:1719–1724. [PubMed: 17014322]
48. Isaac DI, Meyer EG, Kopke KS, Haut RC. Chronic changes in the rabbit tibial plateau following blunt trauma to the tibiofemoral joint. J Biomech. 2010; 43:1682–1688. [PubMed: 20399435]
49. Oegema TR, Carpenter RJ, Hofmeister F, Thompson RC. The interaction of the zone of calcified cartilage and subchondral bone in osteoarthritis. Microscopy Research and Technique. 1997; 37:324–332. [PubMed: 9185154]
50. Chang DG, Iverson EP, Schinagl RM, et al. Quantitation and localization of cartilage degeneration following the induction of osteoarthritis in the rabbit knee. Osteoarthritis Cartilage. 1997; 5:357–372. [PubMed: 9497942]
51. Yosipovitch ZH, Glimcher MJ. Articular Chondrocalcinosis, Hydroxyapatite Deposition Disease, in Adult Mature Rabbits. J Bone Joint Surg Am. 1972; 54:841–853. [PubMed: 5055172]
52. Roemhildt ML, Beynnon B, Anderson K. Effect of Mineralization on the Material Properties of Articular Cartilage in the Rat. Osteoarthritis and cartilage / OARS, Osteoarthritis Research Society. 2011; 19:S15–S16.
53. Fuerst M, Niggemeyer O, Lammers L, et al. Articular cartilage mineralization in osteoarthritis of the hip. BMC Musculoskeletal Disorders. 2009; 10:166. [PubMed: 20038300]
54. Julkunen P, Harjula T, Iivarinen J, et al. Biomechanical, biochemical and structural correlations in immature and mature rabbit articular cartilage. Osteoarthritis Cartilage. 2009; 17:1628–1638. [PubMed: 19615962]
55. Todd Allen R, Robertson CM, Harwood FL, et al. Characterization of mature vs aged rabbit articular cartilage: analysis of cell density, apoptosis-related gene expression and mechanisms controlling chondrocyte apoptosis. Osteoarthritis Cartilage. 2004; 12:917–923. [PubMed: 15501408]
56. Meachim G. Age changes in articular cartilage. 1969. Clin Orthop Relat Res. 2001:S6–13. [PubMed: 11603725]
57. Roemhildt ML, Gardner-Morse M, Rowell C, et al. Gait alterations in rats following attachment of a device and application of altered knee loading. J Biomech. 2010; 43:3227–3231. [PubMed: 20739023]

58. Bove SE, Calcaterra SL, Brooker RM, et al. Weight bearing as a measure of disease progression and efficacy of anti-inflammatory compounds in a model of monosodium iodoacetate-induced osteoarthritis. Osteoarthritis Cartilage. 2003; 11:821–830. [PubMed: 14609535]

59. Clarke KA, Heitmeyer SA, Smith AG, Taiwo YO. Gait Analysis in a Rat Model of Osteoarthrosis. Physiology & Behavior. 1997; 62:951–954. [PubMed: 9333186]

60. O'Connor BL, Visco DM, Heck DA, et al. Gait alterations in dogs after transection of the anterior cruciate ligament. Arthritis Rheum. 1989; 32:1142–1147. [PubMed: 2775322]

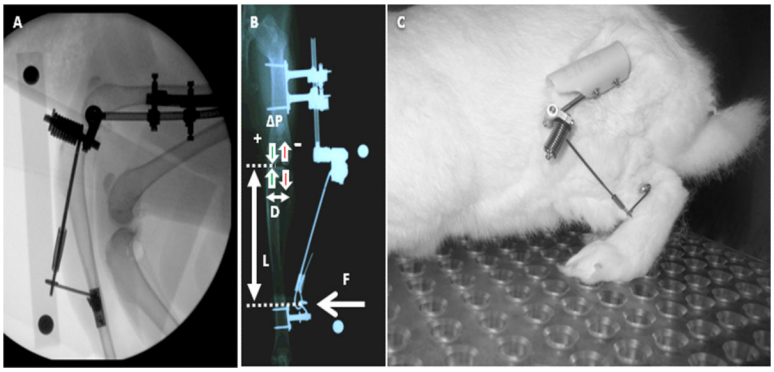

Fig. 1.

A) Fluoroscopy image of a rabbit hind limb showing attachment of the VLD to the bone plates on the lateral femur and tibia and alignment of the axis of rotation of the pivot bearing with the femoral transepicondylar axis. B) AP radiograph illustrating application of varus force to the tibia resulting in increased loading to the medial compartment and decreased loading to the lateral compartment. C) Rabbit with VLD attached and engaged.

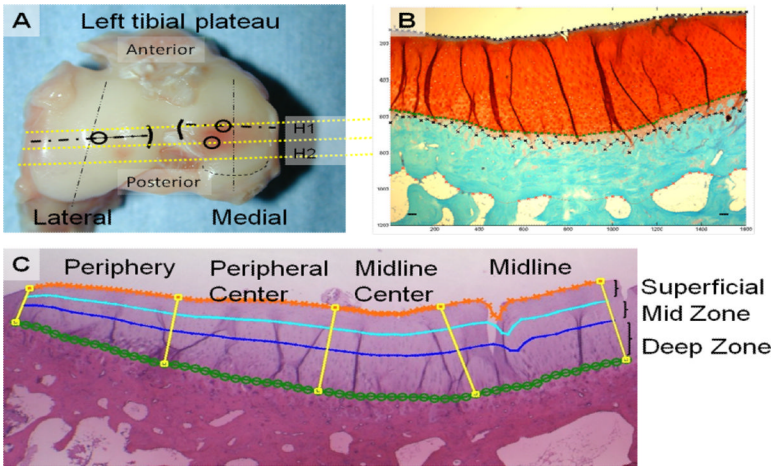

Fig. 2.

A) Superior view of a tibial plateau showing the sites for mechanical testing (?) and histological sections (H1, H2). B) SOFG stained coronal section illustrating measurement of articular cartilage, calcified cartilage, and subchondral bone thicknesses. C) Photomicrograph illustrating regions within each compartment (peripheral, peripheral-central, midline-central and midline) and 3 zonal-depths (superficial (0–25%), mid (25–50%), and deep (50–100%)).

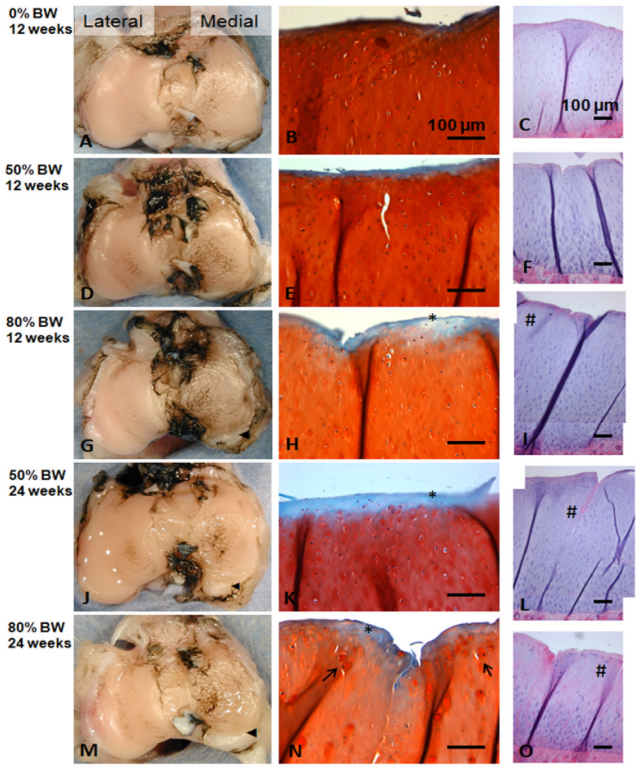

Fig. 3.

Superior views of plateaus stained with India ink indicating mild/moderate fibrillation of the articular surface in the medial compartment and intact surface in the lateral compartment (A, D, G, J, M); ◀ indicates osteophyte/chondrophyte formation in posterior region of the medial compartment. Safranin-O stained histological sections of the superficial and mid zones of the medial compartment (B, E, H, K, N); * indicates loss of proteoglycan staining; → indicates chondrocyte hypertrophy. Full- thickness osteochondral sections of the medial compartment (H&E stain) (C, F, I, L O); # indicates regions of diminished cartilage cellularity with loading. Enlarged images of panels C and O appear in the supplemental data (Figs. S1 & S2).

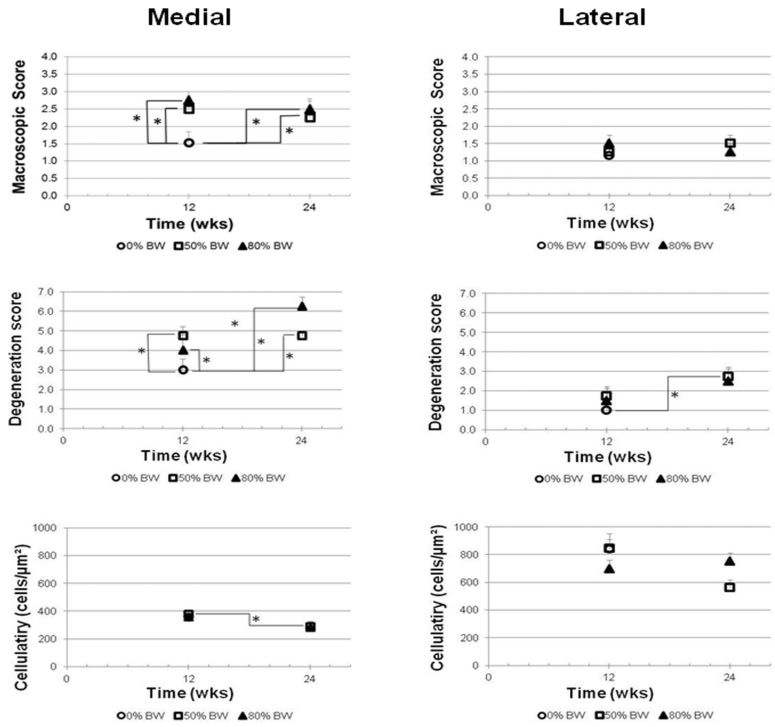

Fig. 4.

Macroscopic scoring of articular cartilage, OARSI degeneration score, and mean cellularity of the medial and lateral compartments of the tibia plateau-experimental limb. * indicates significant difference between groups ($p \leq 0.05$).

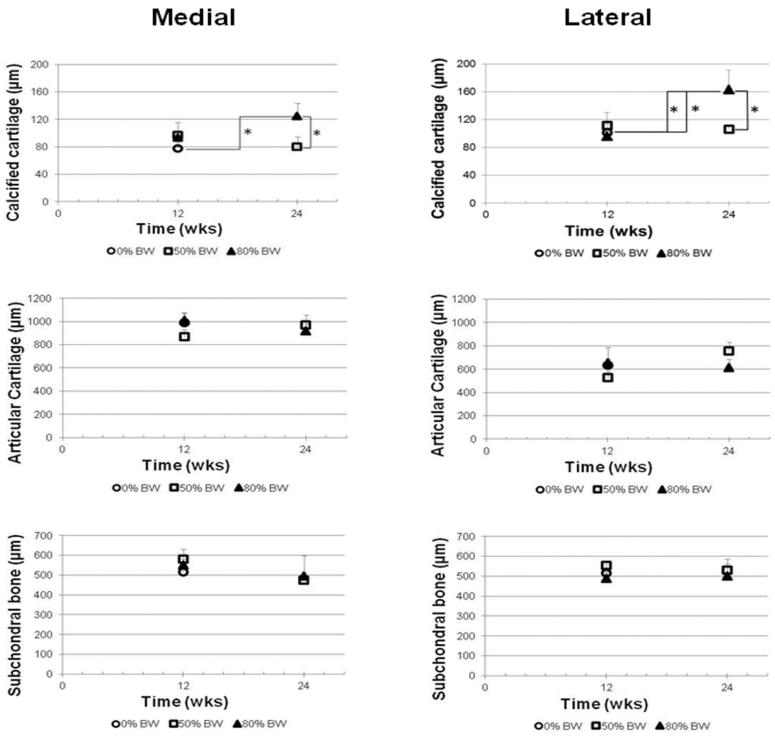

Fig. 5.

Thicknesses of the calcified cartilage, articular cartilage, and subchondral bone for the medial and lateral compartments. * indicates significant difference between groups ($p \leq 0.05$).

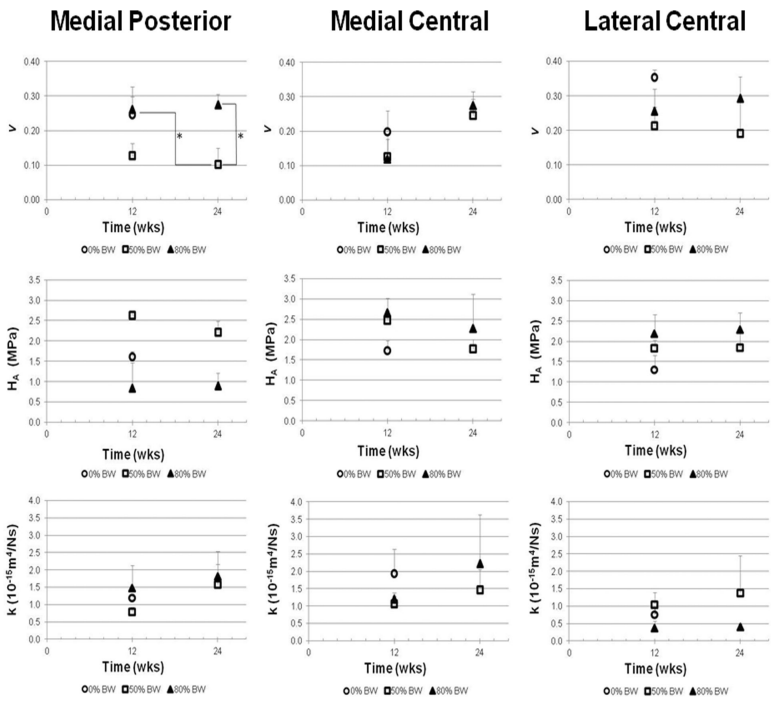

Fig. 6.

Mean Poisson's ratio, aggregate modulus, and permeability of the articular cartilage of the medial and lateral compartments. * indicates significant difference between groups ($p \leq 0.05$).

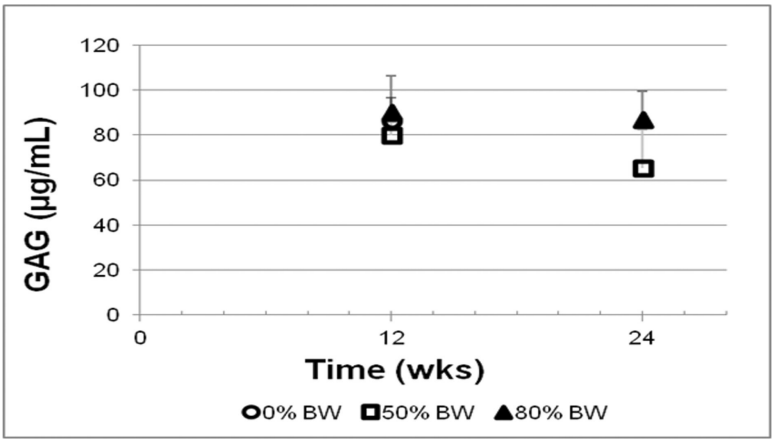

Fig. 7.
Glycosaminoglycan (GAG) content in synovial fluid of the tibiofemoral joint-experimental limb.